Bioorganic & Medicinal Chemistry Letters 22 (2012) 1226–1229

Contents lists available at SciVerse ScienceDirect

Bioorganic & Medicinal Chemistry Letters

journal homepage: www.elsevier.com/locate/bmcl

# Identification of triazolopyridazinones as potent p38α inhibitors

Brad Herberich [a,*], Claire Jackson [a], Ryan P. Wurz [a], Liping H. Pettus [a], Lisa Sherman [b], Qiurong Liu [b], Bradley Henkle [b], Christiaan J.M. Saris [b], Lu Min Wong [b], Samer Chmait [c], Matthew R. Lee [c], Christopher Mohr [c], Faye Hsieh [d], Andrew S. Tasker [a]

[a] Department of Chemistry Research and Discovery, Amgen Inc., One Amgen Center Drive, Thousand Oaks, CA 91320, USA
[b] Department of Inflammation, Amgen Inc., One Amgen Center Drive, Thousand Oaks, CA 91320, USA
[c] Department of Molecular Structure, Amgen Inc., One Amgen Center Drive, Thousand Oaks, CA 91320, USA
[d] Department of Pharmacokinetics and Drug Metabolism, Amgen Inc., One Amgen Center Drive, Thousand Oaks, CA 91320, USA

ARTICLE INFO

*Article history:*
Received 14 October 2011
Revised 14 November 2011
Accepted 18 November 2011
Available online 23 November 2011

*Keywords:*
p38
Kinase
Inflammation

ABSTRACT

Structure–activity relationship (SAR) investigations of a novel class of triazolopyridazinone p38α mitogen activated protein kinase (MAPK) inhibitors are disclosed. From these studies, increased in vitro potency was observed for 2,6-disubstituted phenyl moieties and *N*-ethyl triazolopyridazinone cores due to key contacts with Leu108, Ala157 and Val38. Further investigation led to the identification of three compounds, **3g**, **3j** and **3m** that are highly potent inhibitors of LPS-induced MAPKAP kinase 2 (MK2) phosphorylation in 50% human whole blood (hWB), and possess desirable in vivo pharmacokinetic and kinase selectivity profiles.



The production of TNFα and other cytokines is triggered through the activation of p38α mitogen-activated protein (MAP) kinase by multiple external stimuli including stress and a variety of cytokines.[1] Excessive production of cytokines has been implicated in many chronic inflammatory diseases, such as rheumatoid arthritis and psoriasis. Although there are a number of marketed anti-tumor necrosis factor α (TNFα) biological therapies, including etanercept, adalimumab and infliximab, that provide relief from the symptoms of several inflammatory diseases,[2] researchers have long sought an orally available small molecule that decreases cytokine production by the inhibition of p38α.[3] Earlier efforts from our p38 program at Amgen have focused on pyrazolopyridinones (**1**, Fig. 1) and triazolopyridines **2**.[4] In this communication, we outline our development of a novel class of triazolopyridazinone-derived p38α inhibitors (**3**, Fig. 1) designed to combine the excellent potency and pharmacokinetic profiles of compounds **1** and **2**.

Previous SAR investigations of **1** and **2** demonstrated a cyclopropyl ring to be the optimum amide substitutent;[4] we therefore

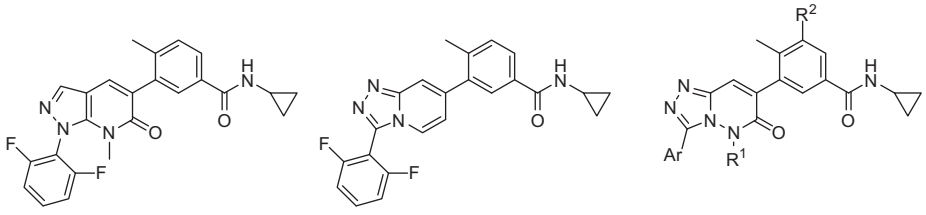


**1**
p38α $IC_{50}$ = 2.3 nM
Rat CL = 220 mL/h/kg

**2**
p38α $IC_{50}$ = 2.5 nM
Rat CL = 370 mL/h/kg

**3**

**Figure 1.** Pyrazolopyridinone-, triazolopyridine- and triazolopyridazinone-derived p38α inhibitors.

* Corresponding author.
*E-mail address:* brad.herberich@amgen.com (B. Herberich).

0960-894X/$ - see front matter © 2011 Elsevier Ltd. All rights reserved.
doi:10.1016/j.bmcl.2011.11.067

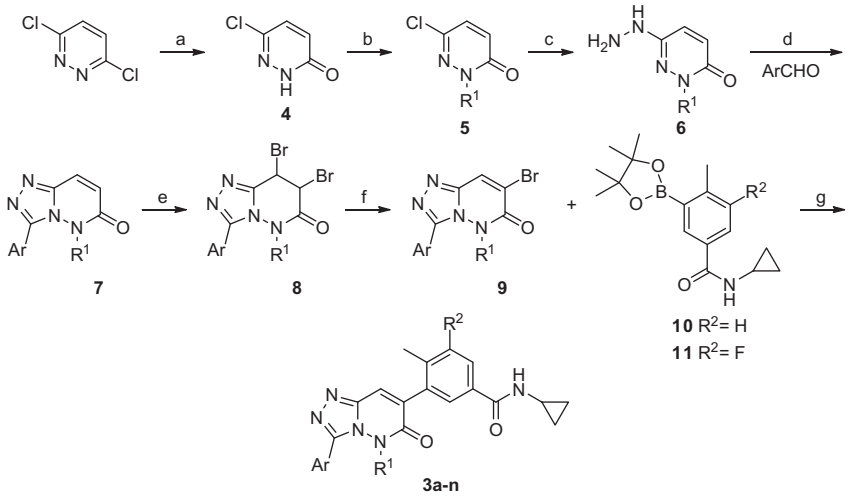

**Scheme 1.** General synthetic scheme towards triazolopyridazinone benzamides **3a–n**. Reagents and conditions: (a) NaOH, $H_2O$, 80 °C, 85%; (b) MeI or EtI, $K_2CO_3$, DMF, 65–98%; (c) hydrazine hydrate, 70 °C, 30–48%; (d) (i) EtOH, reflux, (ii) chloramine T hydrate, THF, 65 °C, 57–82%; (e) $Br_2$, AcOH, 80 °C, 47–95%; (f) $NEt_3$, THF, 60–95%; (g) $PdCl_2(PPh_3)_2$, 2 M $Na_2CO_3$ (aq), dioxane, 120 °C, 26–73%.

focused our present efforts on an investigation of triazolopyridazinone core, tolyl ring, and aryl ring substituents ($R^1$, $R^2$ and Ar, Fig. 1).

Scheme 1 outlines the synthesis of triazolopyridazinones (**3a–n**) starting from commercially available 3,6-dichloropyridazine. Hydrolysis under basic aqueous conditions gave pyridazinone **4**. N-alkylation of the resultant pyridazinone with methyl or ethyl iodide and subsequent $S_NAr$ displacement of the chloride with hydrazine hydrate afforded **6**. The triazolopyridazinone core **7** was prepared by condensation of **6** with a substituted benzaldehyde to form the corresponding hydrazone followed by oxidative cyclization in the presence of chloramine T.[5] Dibromination of **7** followed by mono-debromination under basic conditions gave the desired α-bromide **9**. The synthesis of **3a–n** was subsequently completed via Suzuki coupling with boronic esters **10** or **11**.[6,7]

The in vitro potency of **3a–n** was evaluated by measuring the inhibition of activating transcription factor 2 (ATF2) phosphorylation by p38α as well as the inhibition of TNFα-induced IL-8 production in 50% human whole blood (hWB).[4a] For advanced compounds, on-mechanism activity was verified by measuring their ability to modulate LPS-driven MAPKAP kinase 2 (MK2) phosphorylation in 50% human whole blood, an event that is currently understood to be mediated solely by p38 MAP kinase.[8] The influence of the triazolopyridazinone 3-substitutent on p38α activity was first investigated with compounds **3a–e** (Table 1). The 2,6-disubstituted analogs (**3a–c**) exhibited greater potency in the p38α enzyme and TNFα/IL8 human whole blood assays relative to the corresponding 2,4- or 2,5-disubstitued analogs (**3d–e**). This increase in activity for the 2,6-substituted analogs may be a result of a better van der Waals contacts with Leu108 and Ala157 of p38α (see Fig. 2).

Further SAR studies concerning substitution of the tolyl ring and at N5 of the triazolopyridazinone core are outlined in Table 2. Introduction of a fluorine on the tolyl ring of **3a** (2,6-di-F-Ph) and **3b** (2-Cl-6-F-Ph) to give **3f** and **3g** resulted in improved cell-shifts and an increase of potency in the human whole blood assay. In general, increasing the steric bulk at N5 from methyl to ethyl increased the activity of the compounds (**3i–j** vs **3a,b**) in both the enzyme and human whole blood TNFα/IL-8 assays, a result which can be understood by the ability of the methyl terminus of the ethyl group to engage the side chain of Val38; while the methyl group is unable to form similar contacts (see Fig. 2). The increase in potency with the ethyl substitution at N5 was also observed in the fluorinated tolyl ring analogs (**3l–n** vs **3f–h**). The compounds in Table 2 were evaluated in the LPS/pMK2 assay. When the $R^1$ and $R^2$ substituents were kept constant, the 2-Cl-6-F-phenyl-substituted analogs (**3g**, **3j** and **3m**) exhibited greater activity than the corresponding 2,6-di-F-phenyl (**3f**, **3i** and **3l**) or 2-Me-6-F-phenyl (**3h**, **3k**, **3n**) substituted analogs.

A crystal structure of the unphosphorylated p38/**3j** complex reveals hydrogen bond interactions between the carbonyl of the cyclopropyl amide and Asp168, and between NH of the cyclopropyl amide and Glu71.[9] Similar to pyrazolopyridinone-derived inhibi-

**Table 1**
SAR of modifications of Ar[a]

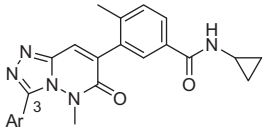

| Compound | Ar | $IC_{50}$ (nM) | |
|---|---|---|---|
| | | p38α | hWB TNFα/IL-8 |
| **3a** | 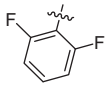 | 1.3 ± 0.2 | 21.4 ± 0.9 |
| **3b** | 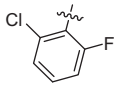 | 1.4 ± 0.4 | 8.5 ± 1.5 |
| **3c** | 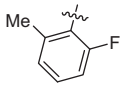 | 2.0 ± 0.6 | 11.3 ± 6.0 |
| **3d** | 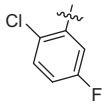 | 6.3 ± 2.0 | 51.7 ± 5.8 |
| **3e** | 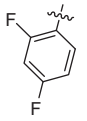 | 16.9 ± 5.3 | 112 ± 40.4 |

[a] The $IC_{50}$ data are mean values derived from at least three independent dose–response curves ± standard deviation.

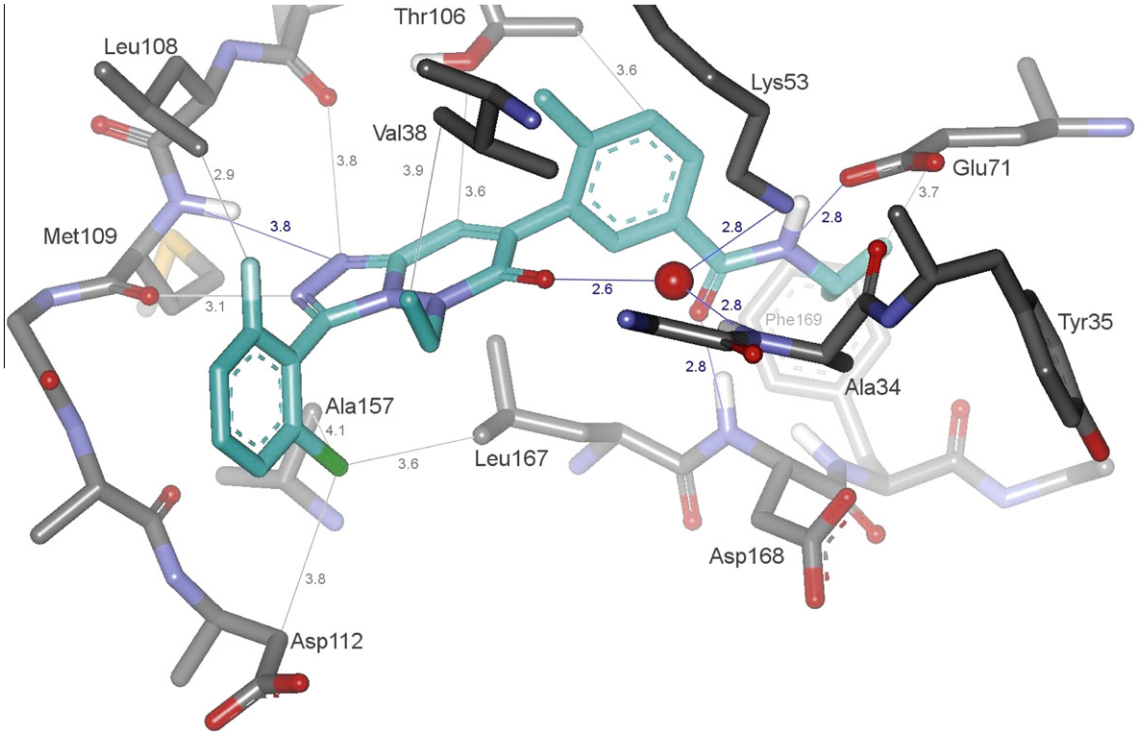


**Figure 2.** X-ray crystal structure of **3j** with unphosphorylated p38α.

tors and in contrast to phthalazine-derived inhibitors,[4a,10] the *N*-ethylpyridinone core induces a reorganization of the P-loop. The carbonyl of the triazolopyridazinone ring participates in a water mediated hydrogen bond to the backbone NH of Ala34 and to the ammonium terminus of Lys53. The methyl group of the tolyl ring sits between the side chains of Thr106 and Val38, while the ethyl group of the *N*-ethylpyridazinone makes contact with Val38. The cyclopropyl group resides next to Phe169. The 2-chloro-6-fluoro phenyl ring is perpendicular to the triazolopyridazinone core and the fluorine group interacts with the side chain of Leu108, while the chloride substituent engages Ala157. An alanine residue on the floor of the ATP binding site is present in only seven kinases within the kinome.[11] Hence, by effectively exploiting both features of Ala157 and Thr106 (a relatively small gatekeeper) compound **3j** is highly selective against a broad panel of kinases (see below).

To evaluate its kinase selectivity, compound **3j** was tested against 442 kinases at a concentration of 10 μM using the Ambit Biosciences Kinomescan.[12] This experiment showed that **3j** had moderate binding (POC <50%) to only one kinase, RET (V804M)[13] (14% of control), outside the p38α, β, and γ isoforms (0, 0, 14% of control, respectively).

The in vivo pharmacokinetic profiles of **3g**, **3j** and **3m** are shown in Table 3. Fluorination of the tolyl ring had little impact on the pharmacokinetic properties of the analogs (**3m** vs **3j**). Exchanging a methyl for an ethyl group on the triazolopyridazinone core increased the exposure and bioavailability (**3g** vs **3m**).

Compounds **3g**, **3j** and **3m** were subjected to CYP3A4 and CYP2D6 inhibition assays as inhibition of these enzymes had been observed by related *N*-ethyl pyrazolopyridinone analogs.[4a] The 3-fluorotolyl analogs **3m** and **3g** showed low CYP3A4 inhibition with an estimated $IC_{50}$ of 11.8 and 25.8 μM, respectively while **3j** possessed an estimated $IC_{50}$ of >27 μM. All three compounds demonstrated an estimated $IC_{50}$ of >27 μM against CYP2D6. Compounds **3g**, **3j** and **3m** were tested for hERG binding through a $^{3}$H-dofetilide

**Table 2**
SAR modifications of Ar, $R^1$, and $R^2$

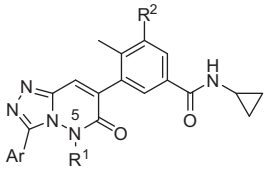


| Compound | Ar | $R^1$ | $R^2$ | $IC_{50}$ (nM) | | |
|---|---|---|---|---|---|---|
| | | | | p38α[a] | hWB TNFα/IL-8[a] | pMK2[b] |
| **3f** | 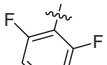 | Me | F | 4.1 ± 3.0 | 7.2 ± 1.8 | 18.5 |
| **3g** | 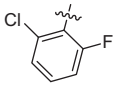 | Me | F | 1.1 ± 0.6 | 2.6 ± 0.001 | 9.8 |
| **3h** | 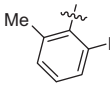 | Me | F | 2.8 ± 0.4 | 12.3 ± 2.6 | 18.0 |
| **3i** | 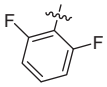 | Et | H | 1.0 ± 0.1 | 4.8 ± 2.2 | 7.8 |
| **3j** | 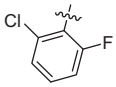 | Et | H | 1.0 ± 0.3 | 3.2 ± 0.9 | 4.9 |
| **3k** | 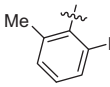 | Et | H | 1.6 ± 0.4 | 14.1 ± 11.7 | 15.8 |
| **3l** | 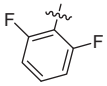 | Et | F | 1.9 ± 0.3 | 3.9 ± 1.5 | 8.0 |

**Table 2** (*continued*)

| Compound | Ar | R[1] | R[2] | $IC_{50}$ (nM) | | |
|---|---|---|---|---|---|---|
| | | | | p38α[a] | hWB TNFα/IL-8[a] | pMK2[b] |
| **3m** | 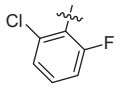 | Et | F | 1.2 ± 0.2 | 1.6 ± 0.4 | 6.9 |
| **3n** | 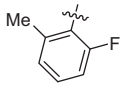 | Et | F | 1.0 ± 0.1 | 3.4 ± 2.1 | 13.6 |

[a] The $IC_{50}$ data are mean values derived from at least three independent dose–response curves ± standard deviation.
[b] The pMK2 $IC_{50}$ data are an average of two values.

**Table 3**
Pharmacokinetic profiles of selected compounds in male Sprague–Dawley rats[a]

| Cmpd | IV (2.0 mg/kg in DMSO) | | | PO (2.0 mg/kg)[b] | |
|---|---|---|---|---|---|
| | CL (mL/h/kg) | $V_{dss}$ (mL/kg) | $t_{1/2}$ (h) | AUC (0–∞) (ng·h/mL) | *F* (%) |
| **3g** | 526 | 2423 | 3.40 | 3190 | 83 |
| **3j** | 787 | 2545 | 2.76 | 1423 | 55 |
| **3m** | 686 | 2704 | 2.76 | 1370 | 42 |

[a] Values are for an average of three rats.
[b] Vehicle: 1% Pluronic F68, 1% HPMC, 15% hydroxypropyl β-cyclodextrin, 83% water.

displacement assay. All three compounds had $IC_{50}$ values of >30 μM.

In conclusion, a new class of triazolopyridazinone p38α inhibitors, based on earlier pyrazolopyridinone and triazolopyridine scaffolds, was designed and synthesized. SAR investigations of the aryl group at the 3-position of the triazolopyridazinone led to the identification of the 2-chloro-6-fluoro-phenyl substituent, which makes contacts with Leu108 and Ala157, and results in analogs possessing superior p38α inhibitory activity in whole cells. Further optimization of related compounds resulted in the preparation of **3g**, **3j**, and **3m**, which displayed single digit nanomolar potency in the huWB LPS/pMK2 assay, favorable pharmacokinetic profiles, high selectivity against other kinases, and low CYP and hERG inhibition.

## Supplementary data

Supplementary data (X-ray crystallography) associated with this article can be found, in the online version, at doi:10.1016/j.bmcl.2011.11.067.

## References and notes


1. Han, J.; Lee, J. D.; Bibbs, L.; Ulevitch, R. J. *Science* **1994**, *265*, 808.
2. Palladino, M. A.; Bahjat, F. R.; Theodorakis, E. A.; Moldawer, L. L. *Nat. Rev. Drug Disc.* **2003**, *2*, 736.
3. (a) Bongartz, T.; Sutton, A. J.; Sweeting, M. J.; Buchan, I.; Matteson, E. L.; Montori, V. *J. Am. Med. Assoc. (JAMA)* **2006**, *295*, 2275; (b) Smolen, J. S.; Aletaha, D.; Koeller, M.; Weisman, M. H.; Emery, P. *Lancet* **2007**, *370*, 1861.
4. (a) Pettus, L. H.; Wurz, R. P.; Xu, S.; Herberich, B.; Henkle, B.; Liu, Q.; McBride, H. J.; Mu, S.; Plant, M. H.; Saris, C. J. M.; Sherman, L.; Wong, L. M.; Chmait, S.; Lee, M. R.; Mohr, C.; Hsieh, F.; Tasker, A. S. *J. Med. Chem.* **2010**, *53*, 2973; (b) Zhang, D.; Tasker, A.; Sham, K. K. C.; Chakrabarti, P. P.; Falsey, J. R.; Herberich, B. J.; Pettus, L. H.; Rzasa, R. M. WO 2008045393, 2008.
5. (a) Thiel, O. R.; Achmatowicz, M. M.; Reichelt, A.; Larsen, R. D. *Angew. Chem., Int. Ed.* **2010**, *49*, 8395; (b) Reichelt, A.; Falsey, J. R.; Rzasa, R. M.; Thiel, O. R.; Achmatowicz, M. M.; Larsen, R. D.; Zhang, D. *Org. Lett.* **2010**, *12*, 792.
6. For syntheses of boronic esters **10** and **11** see: Aston, N. M.; Bamborough, P.; Buckton, J. B.; Edwards, C. D.; Holmes, D. S.; Jones, K. L.; Patel, V. K.; Smee, P. A.; Somers, D. O.; Vitulli, G.; Walker, A. L. *J. Med. Chem.* **2009**, *52*, 6257.
7. *Procedures for the preparation of* ***3j***: A suspension of 3,6-dichloropyridazine (25.50 g, 171.2 mmol) in 100 mL of water was treated with NaOH (15.06 g, 376.6 mmol) and heated at 80 °C for 2 h. The resulting red solution was allowed to cool to rt and was then acidified to pH 1 with concentrated HCl (aq). The off-white solid was washed with water and $Et_2O$ and then dried under vacuum overnight to afford 6-chloropyridazin-3(2*H*)-one (**4**, 19.13 g, 85% yield). A mixture of **4** (2.55 g, 19.54 mmol) and EtI (1.88 mL, 23.44 mmol) in 10 mL of DMF at rt was treated with $K_2CO_3$ (8.10 g, 58.61 mmol). The reaction mixture stirred 48 h at rt and then $H_2O$ was added and the mixture was extracted with EtOAc. The combined organic layers were washed with water, dried over $Na_2SO_4$, filtered and concentrated to give 6-chloro-2-ethylpyridazin-3(2*H*)-one (**5**, 2.70 g, 87% yield). A solution of **5** (2.70 g, 17.03 mmol) in hydrazine hydrate (4.14 mL, 85.13 mmol) was heated at 70 °C. After 2 h, the reaction mixture was loaded directly on to a silica gel column and eluted with 0–10% MeOH in $CH_2Cl_2$ to afford 2-ethyl-6-hydrazinylpyridazin-3(2*H*)-one (**6**, 1.26 g, 48% yield) as a light-yellow solid. A mixture of **6** (163 mg, 1.06 mmol) and 2-chloro-6-fluorobenzaldehyde (168 mg, 1.06 mmol) in 8 mL of EtOH was heated to reflux. After 1 h, the reaction mixture was concentrated, the solid was resuspended in THF (8 mL) and chloramine T-hydrate (265 mg, 1.16 mmol) was added. The mixture was heated at 65 °C for 4 h. The reaction mixture was allowed to cool to rt and $H_2O$ was added. The mixture was extracted with EtOAc. The combined organic layers were dried over anhydrous $Na_2SO_4$, filtered and concentrated. The crude material was purified by silica gel chromatography (0–50% EtOAc in hexanes) to afford 3-(2-chloro-6-fluorophenyl)-5-ethyl-[1,2,4]triazolo[4,3-*b*]pyridazin-6(5*H*)-one (**7**, 222 mg, 72% yield). A mixture of **7** (222 mg, 0.76 mmol) and $Br_2$ (0.19 mL, 3.79 mmol) in 3 mL of acetic acid was heated at 80 °C for 2 h. The reaction was cooled to rt, water was added and the mixture was extracted with EtOAc. The combined organic layers were washed with $H_2O$ and saturated $NaHCO_3$ (aq) and then dried over anhydrous $Na_2SO_4$, filtered and concentrated to afford 7,8-dibromo-3-(2-chloro-6-fluorophenyl)-5-ethyl-7,8-dihydro-[1,2,4]triazolo[4,3-*b*]pyridazin-6(5*H*)-one (**8**, 285 mg, 83% yield) as a yellow oil. A solution of **8** (285 mg, 0.63 mmol) in 3 mL of THF at rt was treated with $NEt_3$ (0.26 mL, 1.89 mmol). After 1 h, $H_2O$ was added and the mixture was extracted with EtOAc. The combined organic layers were dried over anhydrous $Na_2SO_4$, filtered and concentrated to give 7-bromo-3-(2-chloro-6-fluorophenyl)-5-ethyl-[1,2,4]triazolo[4,3-*b*]pyridazin-6(5*H*)-one (**9**, 194 mg, 83% yield) as a yellow oil. In a microwave tube was placed **9** (194 mg, 0.52 mmol), **10** (190 mg, 0.63 mmol), $PdCl_2(PPh_3)_2$ (18 mg, 0.026 mmol) and 2 M $Na_2CO_3$ (aq, 1.3 mL, 2.6 mmol) and 2.5 mL of dioxane. The mixture was heated in a microwave at 120 °C for 25 min. After cooling to rt, $H_2O$ was added and the mixture was extracted with EtOAc. The combined organic layers were dried over anhydrous $Na_2SO_4$, filtered and concentrated. The crude material was purified by HPLC (Phenomenex 150 × 30 mm Luna column) eluting with 5–100% $CH_3CN$ in water with 0.1% TFA at 35 mL/min over 15 min to afford 3-(3-(2-chloro-6-fluorophenyl)-5-ethyl-6-oxo-5,6-dihydro-[1,2,4]triazolo[4,3-*b*]pyridazin-7-yl)-*N*-cyclopropyl-4-methylbenzamide (**3j**, 69 mg, 28% yield) as an off-white solid. $^1$H NMR (400 MHz, $CDCl_3$) $\delta$ 7.81 (s, 1H), 7.75 (dd, $J$ = 7.92, 1.86 Hz, 1H), 7.67 (d, $J$ = 1.76 Hz, 1H), 7.61 (td, $J$ = 8.31, 5.87 Hz, 1H), 7.46 (d, $J$ = 8.02 Hz, 1H), 7.37 (d, $J$ = 8.02 Hz, 1H), 7.25–7.30 (m, 1H), 6.34 (br s, 1H), 4.29 (dq, $J$ = 14.79, 7.13 Hz, 1H), 3.91–4.02 (m, 1 H), 2.90 (tq, $J$ = 7.02, 3.47 Hz, 1H), 2.33 (s, 3H), 1.04 (t, $J$ = 7.04 Hz, 3 H), 0.83–0.90 (m, 2H), 0.58–0.65 (m, 2H). $^{19}$F NMR (400 MHz, $CDCl_3$) $\delta$ −105.90. MS (ESI, pos. ion) *m*/*z*: 466.0 (M+1).
8. Haar, E. *Structure* **2003**, *11*, 611.
9. The X-ray coordinates have been deposited in the RCSB Protein Data Bank database, RCSB ID code: rcsb068453 and PDB ID code: 3U8W). See Supplementary data for crystallographic protocol and refinement statistics.
10. Herberich, B.; Cao, G.-Q.; Chakrabarti, P.; Falsey, J.; Pettus, L.; Rzasa, R. M.; Reed, A. B.; Reichelt, A.; Sham, K.; Thaman, M.; Wurz, R. P.; Xu, S.; Zhang, D.; Hsieh, F.; Lee, M. R.; Syed, R.; Li, V.; Grosfeld, D.; Plant, M. H.; Henkle, B.; Sherman, L.; Middleton, S.; Wong, L. M.; Tasker, A. S. *J. Med. Chem.* **2008**, *51*, 6271.
11. Only 7 out of the 518 kinases have alanine as the floor reside in ATP binding pocket. Manning, G.; Whyte, D. B.; Martinez, R.; Hunter, T.; Sudarsanam, S. *Science* **2002**, *298*, 1912.
12. Ambit Biosciences: http://www.kinomescan.com/
13. The V804M mutation of the RET kinase has been identified in patients with medullary thyroid cancer.